Self-Assembly of Hollow Organic Nanotubes Driven by Arene Regioisomerism

Juan V. Alegre-Requena,*[a] Raquel P. Herrera,[b] and David Díaz Díaz*[c, d, e]

Arene regioisomerism in low-molecular-weight gelators can be exploited as a tool to modulate the micro-structures of the corresponding xerogel networks by using the three different possible substitution patterns *ortho*, *meta* and *para*. This aromatic regioisomer-driven strategy has been used with a cholesterol-based gelator to prepare hollow self-assembled organic nanotubes (S-ONTs) with inside and outside diameters of ca. 35 and 140 nm, respectively. Electron microscopy imaging and theoretical calculations were employed to rationalize the formation mechanism of these S-ONTs. From the three possible regioisomers, only the *ortho*-disubstituted cholesteryl-based gelator showed the optimal angle and distance between substituents to afford the formation of the cyclic assemblies required for nanotube growth by assembling 30–40 units of the gelator. This study opens fascinating opportunities to expand the synthesis of controllable and unique microstructures by modulating geometrical parameters through aromatic regioisomers.

The creation of self-assembled organic nanotubes (S-ONTs) represents a field of research that has attracted much attention during the last decade.[1,2] In fact, it is gradually becoming the first choice for different applications related to nanotubular structures, such as transmembrane mass transporters, supramolecular hosts for biological systems and nanopipettes, among others.[1–4] Although S-ONTs are normally prepared by precipitation processes, their formation triggered through gelation has also been observed, even though it is much rarer.[5–10] In these cases, the obtained S-ONTs have been employed as templates for the preparation of inorganic nanotubes (using the outer part of the S-ONTs),[5–8] fibers (employing the inner part of the S-ONTs),[9] and light-harvesting systems.[10] A clear advantage of S-ONTs formed during gelation is that they can be readily used without an initial isolation process. Nevertheless, one drawback that hampers the rapid evolution of this field is the lack of organic structures capable of creating S-ONTs during the gel formation process. Among the studies published in this area, a few S-ONTs are formed in organic solvents,[10–15] whereas most examples involve the use of protic solvents (water,[16–18] AcOH[5–8] and alcohols[9,19]) or auxiliary metals.[20]

Moreover, we realized that in many studies related to the formation of S-ONTs, there was a di- or polysubstituted aromatic moiety involved in the process. Since it is known that regioisomerism of aromatic polymeric gelators plays a key role in the structures and properties of the corresponding gels,[21–23] we hypothesized that the substituent's relative position of aromatic gelators used for the preparation of S-ONTs may also trigger morphological changes such as those related to length and diameter of the nano-structures.

Inspired by these observations, and as part of our research program related to the synthesis and applications of supramolecular gels, we found a low-molecular-weight (LMW) gelator[24] containing two cholesterol motifs attached to an aromatic core, which allows for the preparation of three different regioisomeric gelators depending on the relative position of the substituents (Figure 1). It is worth mentioning that cholesterol-based gelators for both polar and apolar solvents are widely represented in the literature.[7,25–31] Hence, we decided to investigate the effects of regioisomerism on the

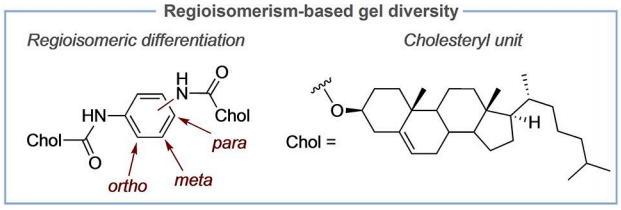

Figure 1. Structure of regioisomeric LMW gelators (**ortho**, **meta**, **para**).

[a] *Dr. J. V. Alegre-Requena*
Department of Chemistry
Colorado State University
Fort Collins, Colorado 80523 (USA)
E-mail: jvalegre@colostate.edu
[b] *Dr. R. P. Herrera*
Instituto de Síntesis Química
y Catálisis Homogénea (ISQCH)
CSIC-Universidad de Zaragoza
C/ Pedro Cerbuna 12, 50009 Zaragoza (Spain)
[c] *Dr. D. Díaz Díaz*
Institut für Organische Chemie
Universität Regensburg
Universitätsstr. 31, 93040 Regensburg (Germany)
E-mail: david.diaz@ur.de
[d] *Dr. D. Díaz Díaz*
Departamento de Química Orgánica
Universidad de La Laguna
Avda. Astrofísico Francisco Sánchez, 38206 La Laguna, Tenerife (Spain)
E-mail: ddiazdiaz@ull.edu.es
[e] *Dr. D. Díaz Díaz*
Instituto Universitario de Bio-Orgánica Antonio González
Universidad de La Laguna
Avda. Astrofísico Francisco Sánchez 2, 38206 La Laguna, Tenerife (Spain)

Supporting information for this article is available on the WWW under https://doi.org/10.1002/cplu.202000473

self-assembly behavior of this molecule. The synthesis of this family of gelators was easily performed via double amidation in one step under mild conditions (Scheme S1). Synthetic and characterization details can be found in the Supporting Information (Figures S1–S4). Gels were obtained in a variety of solvents with different polarities (Table S1). In good agreement with our previous observations made with isomeric ionene gels,[21] the three isomers showed different gelation properties. Specifically, *meta*- (**meta**) and *para*- (**para**) substituted derivatives formed gels in the same solvents upon the classical heating-cooling protocol, whereas the *ortho*- (**ortho**) analogue showed different gelation properties (Table S1 and Figures S5–S9). In order to facilitate further reading, the three isomeric gelators are labeled as **meta**, **para** and **ortho**, respectively. All gels were found to be thermoreversible and, most of them opaque, which suggested the formation of supramolecular aggregates larger than the wavelength of visible light.

Critical gelation concentration (CGC), gelation time (G_t) and *gel*-to-*sol* transition temperature (T_{gel}) of the gels also differed for the different regioisomers at the same concentration (Table S2 and Figure S10). In general, **ortho** gels displayed lower T_{gel} values than its **meta** and **para** analogues. Further comparative studies were made taking 1,4-dioxane and aniline as model solvents. Similar to other physical gels, a decrease of the G_t and an increase of the T_{gel} was observed as the gelator concentration increased (Figure S11). Reversible *gel*-to-*sol* transitions were observed not only thermally but also mechanically upon shaking (Figure S12). The viscoelastic gel nature of the materials (storage modulus $G' >$ loss modulus G'') was confirmed by standard oscillatory rheological measurements including dynamic frequency, strain and time sweep experiments (Figure S13). Higher mechanical strength was found for the **meta** and **para** gels, which revealed a storage modulus approximately one order of magnitude higher than the corresponding **ortho** gel. In addition, comparative FT-IR spectroscopic studies (Figure S14) showed slight shifts in some of the main vibration bands among the three isomers (e.g. $\Delta_{\text{N-H stretching}} \sim 3431$–$3330\ \text{cm}^{-1}$, $\Delta_{\text{C=O stretching}} \sim 1728$–$1726\ \text{cm}^{-1}$, $\Delta_{\text{amide I}} \sim 1707$–$1696\ \text{cm}^{-1}$, $\Delta_{\text{amide II}} \sim 1550$–$1530\ \text{cm}^{-1}$), suggesting that they undergo different rearrangements to form the gel networks. This was further rationalized by computational studies (*vide infra*). Furthermore, intermolecular interaction patterns maintained certain similarities between the bulk isomeric gelators and the corresponding freeze-drying xerogels, suggesting the existence of similar aggregates in both states (Figure S14).

Most interestingly, we found that only the gelator **ortho** formed hollow S-ONTs as demonstrated by electron microscopy imaging of the corresponding xerogels prepared from gels made in dry 1,4-dioxane (Figure 2 and Figure S15). In contrast, thin and wide layers with different aspect ratios were observed in the case of **para** and **meta** xerogels. To the best of our knowledge, this is the first case in which the formation of S-ONTs has been reported in an ether-based solvent. These nanotubes show inside and outside diameters of approximately 35 and 140 nm respectively, and their formation sharply affects the properties of the gels. For instance, the temporal stability of the 1,4-dioxane gels formed is quite different for the three isomers, ranging from one to seven

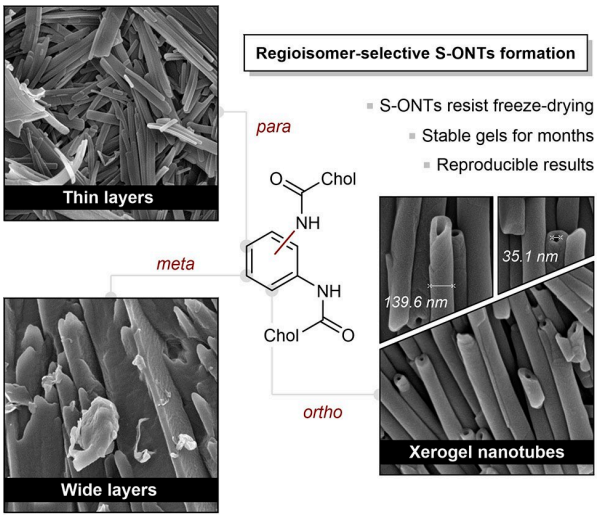

Figure 2. Structural core of the aromatic cholesteryl ester-based regioisomeric gelators (i.e., *ortho*-, *meta*- and *para*- disubstitution pattern) along with field emission scanning electron microscopy (FESEM) images of the corresponding 1,4-dioxane xerogels ($c = 90\ \text{g L}^{-1}$). Chol = cholesteryl.

days for **meta** and **para**-based gels to, at least, several months for the **ortho**-based gel S-ONTs.

In general, the structures observed by FESEM were also in agreement with those obtained by TEM. We checked the reproducibility of the S-ONTs formation using different batches of the xerogels and ensuring that the images were representative of the bulk materials.

We were able to obtain crystals precipitated from 1,4-dioxane gels of **meta** and **para** (Figure 3A). The geometries of these crystals were determined by X-ray crystallography and resulted crucial to understand the most prevalent self-aggregation patterns of this new type of cholesteryl gelators. There are two main differences that influence the self-assembly patterns of both crystals: the orientation of the NH amide bonds and the interactions of the gelators with dioxane. When using **meta**, the two NH groups point towards the same direction and the molecules of dioxane interact with different NH groups and CH groups of the cholesterol moieties. Contrarily, the two NH bonds of **para** molecules are oriented in opposite directions and the molecules of dioxane always interact in the same way with the gelator units, forming O···H–N bonds with two amide groups from different molecules. However, X-ray powder diffraction (XRPD) studies showed some similarities between the crystalline patterns of the isomeric gelators (Figure S16), which was in agreement with the FT-IR observations.

As expected, dispersive interactions between different cholesterol moieties are ubiquitous among both crystals, suggesting that this type of interaction also plays a major role in gel formation (Figure 3B). With this preliminary information, theoretical calculations[32–33] were performed to gain insight into the nanotube formation taking place in **ortho** 1,4-dioxane gels. Computational details and thermochemistry data are included in the Supporting Information. Even though the conformational space is huge in this type of compound, we observed that the cholesteryl units were present in similar geometries in **para** and **meta** crystals. Therefore,

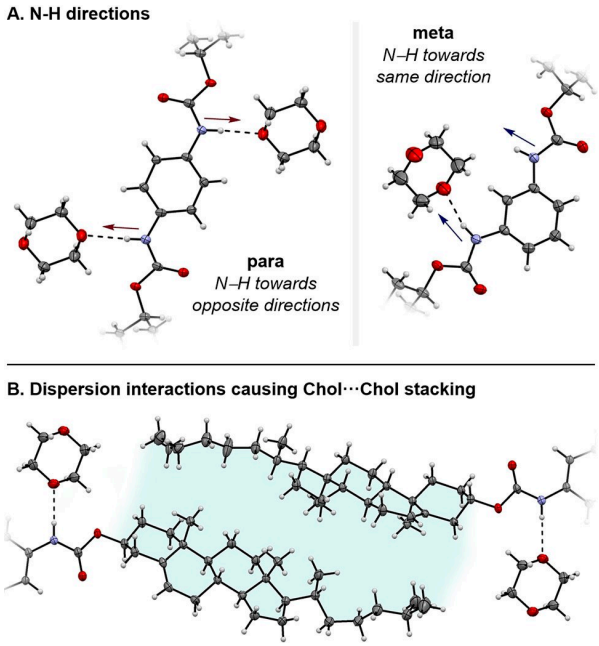

Figure 3. (A) Structures from X-ray crystallography measurements of **para** and **meta** crystals precipitated from 1,4-dioxane gels. The direction of the NH groups is shown with arrows. (B) Intermolecular dispersion interactions created between cholesteryl groups in the crystals (shown in light green). Deposition Number(s) 2019192 (for **meta**) and 2019193 (for **para**) contain the supplementary crystallographic data for this paper. These data are provided free of charge by the joint Cambridge Crystallographic Data Centre and Fachinformationszentrum Karlsruhe Access Structures service www.ccdc.cam.ac.uk/structures.

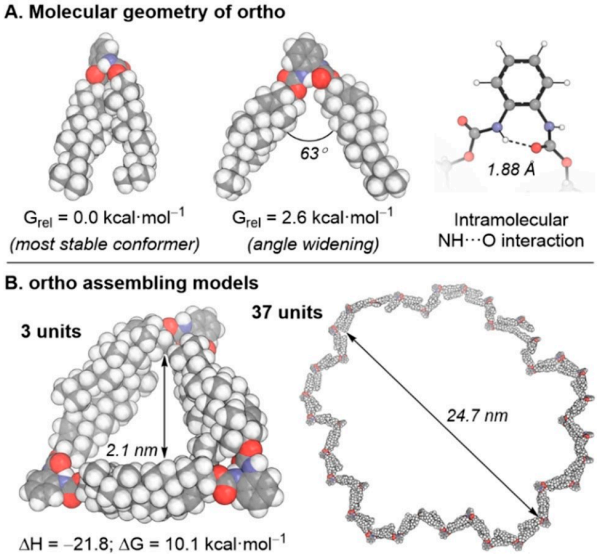

Figure 4. (A) Geometrical parameters of the most stable **ortho** conformers. (B) Cyclic assembling models containing multiple units of **ortho** gelator.

we employed this cholesteryl conformation while changing the orientations of the amide groups during the conformational sampling, obtaining four conformers. Initially, density functional theory (DFT) calculations were carried out at the ωB97X-D/Def2-QZVPP (SMD, solvent = 1,4-dioxane)//ωB97X-D/6-31G(d) level.[34–41] For this study, the use of a functional with dispersion corrections such as ωB97X-D increases the reliability of the results in a great extent due to the great amount of cholesteryl···cholesteryl interactions formed. Additionally, we included a single-point energy correction with a quadruple-zeta basis set (rather than counterpoise corrections) in order to minimize problems related to basis set superposition (BSSE) and incompleteness (BSIE) errors.[42]

In the most stable conformer of **ortho**, the two cholesteryl groups are interacting with each other, leading to a considerably contracted geometry (Figure 4A, left). However, in principle, the stacking of gelator units with this type of geometry does not lead to any viable tubular type of assembly. We found that there are low-lying conformers that present wider angles between the two cholesteryl motifs, creating gelator geometries suitable for the creation of circular patterns. The relatively low Gibbs free energy (G) required to widen the angle of the most stable conformer (2.6 kcal·mol^{-1} to generate an angle of 63°, Figure 4A, middle) could be overcome by the creation of extensive networks of dispersive interactions between cholesteryl units in the gel. The main difference between the most favorable **ortho** geometries and the structures found in **para** and **meta** crystals relies on the creation of an intramolecular NH···O interaction (Figure 4A, right). This interaction found in **ortho** molecules cannot be formed in the other two regioisomers due to the greater distance that separates the two amide groups. The intramolecular H bond might explain why the **ortho** gelator adopts angular geometries that promote the creation of tubular assemblies rather than linear structures as observed in **para** and **meta** crystals.

We used a model consisting in three gelator units to analyse the thermodynamic parameters of **ortho** self-assembly (Figure 4B, left). This is the smallest cyclic assembly in which all the cholesteryl groups are interacting with other cholesteryl motif. The calculated favourable enthalpy (ΔH) of aggregation (−21.8 kcal·mol^{-1}) suggests that the cholesteryl-based dispersive interactions compensate for the energy penalty caused by the angle widening required to adopt cyclic patterns. Furthermore, the unfavourable ΔG value (10.1 kcal·mol^{-1}) indicates that more molecules of gelator are necessary to create larger interaction networks and promote the stable generation of nanotubes, which is common in nucleation processes.[43] A model with four **ortho** units was also tested and we found that the cholesteryl-cholesteryl angle could be expanded to approximately 87° to form a stable cyclic noncovalent complex (Figure S17). Using this gelator units with wider angles, we designed a more realistic macromolecular system that reproduces the inner diameter observed experimentally (commonly from 20 to 40 nm). Since this system was prohibitively large for DFT calculations, we carried out geometry optimizations with semi-empirical methods (PM7)[44] to estimate qualitatively how many **ortho** molecules are required to form realistic tubular assemblies (Figure S18). In this study, 37 units were needed to generate an inner diameter of 24.7 nm (Figure 4B, right), suggesting that at least 30–40 units are required to simulate inner diameters observed in the lower range of the experimental values. It should be emphasized that further experimental evidences[3,4] are still necessary to demonstrate the nanotubular assemblies are formed by 37 units of the **ortho** isomer. Other possibilities such a

rolling of sheeting or coiling of tapes can not be ruled out at this point.[3,4]

In summary, a cholesteryl-based gelator was used to exploit the ability of aromatic regioisomers to modulate the properties of supramolecular gels. Among the three possible regioisomers, only the **ortho** presented suitable structural parameters (i.e. angle and distance between substituents) to yield hollow self-assembled organic nanotubes (S-ONTs) in ether-based solvents. A combination of experimental and computational techniques was employed to study the properties and formation mechanism of these unique S-ONTs. The results of this study open exciting possibilities to generate controllable and exclusive supramolecular architectures by using regioisomer families, which represents a straightforward strategy since in most cases the production of aromatic regioisomers share similar synthetic protocols.

Acknowledgements

Financial support from the Deutsche Forschungsgemeinschaft (DFG, Heisenberg Professorship to D.D.D.), Universität Regensburg and BBVA Foundation (2018 Leonardo Grant for Researchers and Cultural Creators to R.P.H.). R.P.H. also thanks Ministerio de Economía, Industria y Competitividad (MINECO-FEDER CTQ2017-88091-P and RED2018-102471-T) and Gobierno de Aragón-Fondo Social Europeo (Research Group E07_20R) for financial support. J.V.A.-R. thanks the Government of Aragon (DGA) for a predoctoral contract. We acknowledge the Extreme Science and Engineering Discovery Environment (XSEDE) allocation TG-CHE190111. D.D.D. thanks the Spanish Ministry of Science, Innovation and Universities for the Senior Beatriz Galindo Award (Distinguished Researcher; BEAGAL18/00166). D.D.D. thanks NANOtec, INTech, Cabildo de Tenerife and ULL for laboratory facilities. Open access funding enabled and organized by Projekt DEAL.

Conflict of Interest

The authors declare no conflict of interest.

Keywords: gels · nanotubes · regioisomers · self-assembly · supramolecular chemistry

[1] M. Liu, L. Zhang, T. Wang, *Chem. Rev.* **2015**, *115*, 7304–7397.
[2] T. Shimizu, *Bull. Chem. Soc. Jpn.* **2018**, *91*, 623–668.
[3] T. Shimizu, W. Ding, N. Kameta, *Chem. Rev.* **2020**, *120*, 2347–2407.
[4] T. Shimizu, M. Masuda, H. Minamikawa, *Chem. Rev.* **2005**, *105*, 1401–1444.
[5] Y. Ono, K. Nakashima, M. Sano, Y. Kanekiyo, K. Inoue, J. Hojo, S. Shinkai, M. Sano, J. Hojo, *Chem. Commun.* **1998**, 1477–1478.
[6] Y. Ono, K. Nakashima, M. Sano, J. Hojo, S. Shinkai, *J. Mater. Chem.* **2001**, *11*, 2412–2419.
[7] J. H. Jung, H. Kobayashi, M. Masuda, T. Shimizu, S. Shinkai, *J. Am. Chem. Soc.* **2001**, *123*, 8785–8789.
[8] J. H. Jung, S.-H. Lee, J. S. Yoo, K. Yoshida, T. Shimizu, S. Shinkai, *Chem. Eur. J.* **2003**, *9*, 5307–5313.
[9] P. Anilkumar, M. Jayakannan, *J. Phys. Chem. B* **2010**, *114*, 728–736.
[10] N. Kameta, K. Ishikawa, M. Masuda, M. Asakawa, T. Shimizu, *Chem. Mater.* **2012**, *24*, 209–214.
[11] C. F. van Nostrum, R. J. M. Nolte, *Chem. Commun.* **1996**, 2385–2392.
[12] C. Boettcher, B. Schade, J.-H. Fuhrhop, *Langmuir* **2001**, *17*, 873–877.
[13] J. H. Jung, T. Shimizu, S. Shinkai, *J. Mater. Chem.* **2005**, *15*, 3979–3986.
[14] N. Diáz, F.-X. Simon, M. Schmutz, P. Mésini, *Macromol. Symp.* **2006**, *241*, 68–74.
[15] L. Zhang, C. Liu, Q. Jin, X. Zhu, M. Liu, *Soft Matter* **2013**, *9*, 7966–7973.
[16] Q. Ji, R. Iwaura, M. Kogiso, J. H. Jung, K. Yoshida, T. Shimizu, *Chem. Mater.* **2004**, *16*, 250–254.
[17] P. Gao, C. Zhan, M. Liu, *Langmuir* **2006**, *22*, 775–779.
[18] N. Kameta, M. Masuda, T. Shimizu, *ACS Nano* **2012**, *6*, 5249–5258.
[19] M. F. Rizkiana, R. Balamurugan, J. H. Liu, *New J. Chem.* **2015**, *39*, 6068–6075.
[20] V. M. Suresh, A. De, T. K. Maji, *Chem. Commun.* **2015**, *51*, 14678–14681.
[21] J. Bachl, D. Zanuy, D. E. López-Pérez, G. Revilla-López, C. Cativiela, C. Alemán, D. D. Díaz, *Adv. Funct. Mater.* **2014**, *24*, 4893–4904.
[22] P. Duan, X. Zhu, M. Liu, *Chem. Commun.* **2011**, *47*, 5569–5571.
[23] Z. Liu, Y. Jiang, J. Jiang, D. Zhai, D. Wang, M. Liu, *Soft Matter* **2020**, *16*, 4115–4120.
[24] T. Jiao, F. Gao, Y. Wang, J. Zhou, F. Gao, X. Luo, *Curr. Nanosci.* **2012**, *8*, 111–116.
[25] J. C. Wu, T. Yi, Q. Xia, Y. Zou, F. Liu, J. Dong, T. M. Shu, F. Y. Li, C. H. Huang, *Chem. Eur. J.* **2009**, *15*, 6234–6243.
[26] K. Sugiyasu, N. Fujita, S. Shinkai, S. J. Mater, *Chem.* **2005**, *15*, 2747–2754.
[27] J. H. Jong, K. Nakashima, S. Shinkai, *Nano Lett.* **2001**, *1*, 145–148.
[28] J. H. Jong, Y. Ono, S. Shinkai, *Langmuir* **2000**, *16*, 1643–1649.
[29] J. H. Jung, H. Kobayashi, K. J. C. van Bommel, S. Shinkai, T. Shimizu, *Chem. Mater.* **2002**, *14*, 1445–1447.
[30] J. C. Wu, T. Yi, Y. Zou, Q. Xia, T. Shu, F. Liu, Y. H. Yang, F. Y. Li, Z. G. Chen, Z. G. Zhou, C. H. Huang, *J. Mater. Chem.* **2009**, *19*, 3971–3978.
[31] D. D. Díaz, J. J. Cid, P. Vázquez, T. Torres, *Chem. Eur. J.* **2008**, *14*, 9261–9273.
[32] Gaussian 16, Revision C.01, M. J. Frisch, G. W. Trucks, H. B. Schlegel, G. E. Scuseria, M. A. Robb, J. R. Cheeseman, G. Scalmani, V. Barone, G. A. Petersson, H. Nakatsuji, X. Li, M. Caricato, A. V. Marenich, J. Bloino, B. G. Janesko, R. Gomperts, B. Mennucci, H. P. Hratchian, J. V. Ortiz, A. F. Izmaylov, J. L. Sonnenberg, D. Williams-Young, F. Ding, F. Lipparini, F. Egidi, J. Goings, B. Peng, A. Petrone, T. Henderson, D. Ranasinghe, V. G. Zakrzewski, J. Gao, N. Rega, G. Zheng, W. Liang, M. Hada, M. Ehara, K. Toyota, R. Fukuda, J. Hasegawa, M. Ishida, T. Nakajima, Y. Honda, O. Kitao, H. Nakai, T. Vreven, K. Throssell, J. A. Montgomery, Jr., J. E. Peralta, F. Ogliaro, M. J. Bearpark, J. J. Heyd, E. N. Brothers, K. N. Kudin, V. N. Staroverov, T. A. Keith, R. Kobayashi, J. Normand, K. Raghavachari, A. P. Rendell, J. C. Burant, S. S. Iyengar, J. Tomasi, M. Cossi, J. M. Millam, M. Klene, C. Adamo, R. Cammi, J. W. Ochterski, R. L. Martin, K. Morokuma, O. Farkas, J. B. Foresman, D. J. Fox, Gaussian, Inc., Wallingford CT, 2016.
[33] GoodVibes 3.0.1. G. Luchini, J. V. Alegre-Requena, I. Funes-Ardoiz, R. S. Paton, *F1000Research* **2020**, *9*, 291.
[34] A. D. Becke, *J. Chem. Phys.* **1997**, *107*, 8554–8560.
[35] J.-D. Chai, M. Head-Gordon, *Phys. Chem. Chem. Phys.* **2008**, *10*, 6615–6620.
[36] W. J. Hehre, R. Ditchfield, J. A. Pople, *J. Chem. Phys.* **1972**, *56*, 2257–2261.
[37] P. C. Hariharan, J. A. Pople, *Theor. Chim. Acta* **1973**, *28*, 213–222.
[38] F. Weigend, R. Ahlrichs, *Phys. Chem. Chem. Phys.* **2005**, *7*, 3297–3305.
[39] F. Weigend, *Phys. Chem. Chem. Phys.* **2006**, *8*, 1057–1065.
[40] B. Mennucci, E. Cancès, J. Tomasi, *J. Phys. Chem. B.* **1997**, *101*, 10506–10517.
[41] A. V. Marenich, C. J. Cramer, D. G. Truhlar, *J. Phys. Chem. B.* **2009**, *113*, 6378–6396.
[42] R. Sure, S. Grimme, *J. Chem. Theory Comput.* **2015**, *11*, 3785–3801.
[43] S. Karthika, T. K. Radhakrishnan, P. Kalaichelvi, *Cryst. Growth Des.* **2016**, *16*, 6663–6681.
[44] J. J. P. Stewart, *J. Mol. Model.* **2013**, *19*, 1–32.

Manuscript received: June 17, 2020
Revised manuscript received: July 28, 2020